

Cupric Superoxo-Mediated Intermolecular C–H Activation Chemistry

Ryan L. Peterson,^{†,‡} Richard A. Himes,[†] Hiroaki Kotani,[§] Tomoyoshi Suenobu,[§] Li Tian,^{||} Maxime A. Siegler,[†] Edward I. Solomon,^{*,||} Shunichi Fukuzumi,^{*,‡,§} and Kenneth D. Karlin^{*,†,‡}

[†]Department of Chemistry, Johns Hopkins University, Baltimore, Maryland 21218, United States

[‡]Department of Bioinspired Science, Ewha Womans University, Seoul 120-750, Korea

[§]Department of Material and Life Science, Graduate School of Engineering, Osaka University, Suita, Osaka 565-0871, Japan

^{||}Department of Chemistry, Stanford University, Stanford, California 94305, United States

S Supporting Information

ABSTRACT: The new cupric superoxo complex $[\text{LCu}^{\text{II}}(\text{O}_2^{\bullet-})]^+$, which possesses particularly strong O–O and Cu–O bonding, is capable of intermolecular C–H activation of the NADH analogue 1-benzyl-1,4-dihyronicotinamide (BNAH). Kinetic studies indicated a first-order dependence on both the Cu complex and BNAH with a deuterium kinetic isotope effect (KIE) of 12.1, similar to that observed for certain copper monooxygenases.

Copper(I) reactions with molecular oxygen play fundamental roles in many chemical and biological processes.^{1,2} Copper-dependent proteins perform a diverse array of oxidative and oxygenative reactions. This has inspired considerable efforts in the design of novel ligands and copper-coordinated complexes as well as the study of ligand–copper(I) dioxygen adducts to elucidate their structures, electronic characteristics, and substrate reactivities.^{2–4} In comparison with binuclear copper dioxygen-derived species, mononuclear analogues have been synthetically challenging and hence are less well understood.^{3,5} However, they are fundamentally important and directly relevant to copper proteins, including dopamine- β -monooxygenase (D β M) and peptidylglycine- α -hydroxylating monooxygenase (PHM).⁶ These enzymes possess a so-called noncoupled binuclear active site,⁷ which comprises two Cu centers separated by ~ 11 Å. Dioxygen binding and substrate hydroxylation occur at one of the copper sites (designated Cu_M). In an important PHM X-ray structure, a dioxygen-derived species presumed to be an end-on bound cupric superoxide species (i.e., Cu^{II}–O–O^{•-}) resides adjacent to an inhibitory substrate analogue.^{6c} Along with biochemical,^{6a,6b,8} chemical, and computational studies,^{5,9} the cupric superoxo species is thought by many to be the reactive intermediate responsible for initiating oxidation via hydrogen-atom abstraction. However, other species have been considered as important intermediates in enzymatic turnover, either prior to or following substrate attack, including cupric hydroperoxo (Cu^{II}–OOH)¹⁰ and high-valent cupryl (Cu^{II}–O[•] ↔ Cu^{III}=O) entities.^{4b,9c,11}

In our own research program, we seek to elucidate the chemical nature of all of these mononuclear species. In this report, we describe the generation and characterization of a new Cu^{II}(O₂^{•-}) species and an example of substrate C–H activation (i.e., oxidative C–H bond cleavage). To this point, cupric

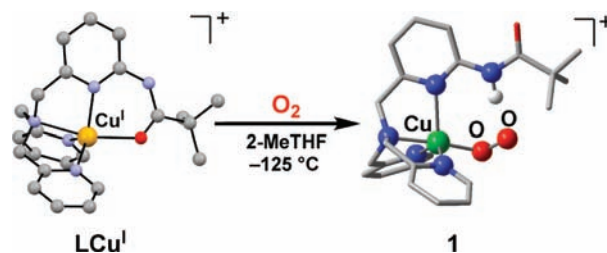


Figure 1. (left) Representation of the cationic portion of the X-ray structure of $[\text{LCu}^{\text{I}}]^+(\text{B}(\text{C}_6\text{F}_5)_4)^-$, revealing the $\text{N}_4\text{O}_{(\text{amide})}$ coordination ($\text{Cu}-\text{O} = 2.190$ Å). (right) Calculated structure (see the Supporting Information) of $[\text{LCu}^{\text{II}}(\text{O}_2^{\bullet-})]^+$ (1), indicating the H-bonding interaction between the ligand and the superoxo β -oxygen atom. See the text for further discussion.

superoxo complexes have been shown to exhibit phenol O–H bond cleavage reactions,^{10a,12} and in one case, Itoh and co-workers¹³ provided evidence for a Cu^{II}(O₂^{•-})-mediated intramolecular benzylic C–H oxygenation. Here, for the first time, an intermolecular C–H substrate oxidation reaction has been achieved, with kinetic data clearly implicating the involvement of the Cu^{II}(O₂^{•-}) complex in rate-limiting substrate C–H bond cleavage.

The Cu^I complex $[\text{LCu}^{\text{I}}]^+$ [as the $\text{B}(\text{C}_6\text{F}_5)_4^-$ salt¹⁴] of a ligand L previously employed by Masuda and co-workers,^{14a} namely, [bis(pyrid-2-ylmethyl){6-(pivalamido)pyrid-2-yl}methyl]amine], was exposed to O₂ (by bubbling via a syringe needle) in 2-methyltetrahydrofuran (MeTHF) solvent at -125 °C to form the adduct $[\text{LCu}^{\text{II}}(\text{O}_2^{\bullet-})]^+$ (1) (Figure 1), which exhibited UV–vis absorptions [$\lambda_{\text{max}} = 410$ nm ($3700 \text{ M}^{-1} \text{ cm}^{-1}$), 585 nm ($900 \text{ M}^{-1} \text{ cm}^{-1}$), 741 nm ($1150 \text{ M}^{-1} \text{ cm}^{-1}$)]¹⁵ characteristic of a mononuclear end-bound Cu^{II} superoxo complex. This temperature well below -80 °C was necessary in order to observe this 1:1 Cu/O₂ adduct. Under these conditions, this green, EPR-silent species was quite stable, decaying only very slowly (half-life > 4 h) with conversion to $[\{\text{LCu}^{\text{II}}\}_2(\text{O}_2^{2-})]^{2+}$ (2), a μ -1,2-peroxodicopper(II) complex [$\lambda_{\text{max}} = 541$ nm ($9900 \text{ M}^{-1} \text{ cm}^{-1}$)] that is observed when $[\text{LCu}^{\text{I}}]^+$ is oxygenated at -80 °C.^{14b}

A resonance Raman (rR) spectrum (77 K, excitation at 413 nm) of 1 in frozen MeTHF solution is shown in Figure 2. The O–O stretch was observed at 1130 cm^{-1} as a single peak

Received: November 21, 2010

Published: January 25, 2011

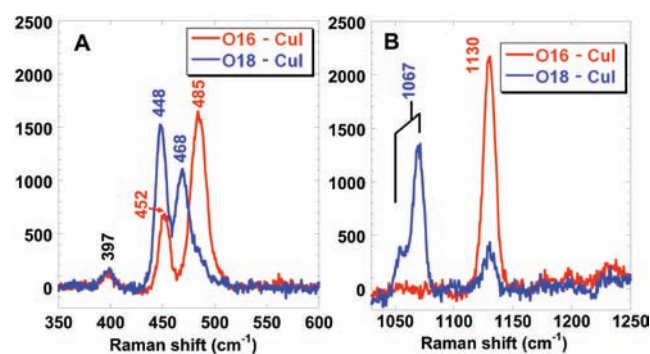


Figure 2. Solvent-subtracted rR spectra of MeTHF solutions of **1** ($\lambda_{\text{ex}} = 413 \text{ nm}$): (A) $\nu(\text{Cu}-\text{O})$ region; (B) $\nu(\text{O}-\text{O})$ region. Red, $^{16}\text{O}_2$; blue, $^{18}\text{O}_2$.

when the complex was formed with $^{16}\text{O}_2$ (Figure 2B, red), but upon $^{18}\text{O}_2$ isotopic substitution, two features were observed (Figure 2B, blue). This behavior is consistent with a Fermi resonance between the $^{18}\text{O}_2$ vibration and a nonenhanced mode at similar energy. From the energy and intensity of the two observed mixed-modal features, the preinteraction energy of the resonantly enhanced $^{18}\text{O}-^{18}\text{O}$ stretch was calculated to be 1067 cm^{-1} . Thus, the O–O stretch was shifted to lower energy by 63 cm^{-1} upon $^{18}\text{O}_2$ substitution, consistent with a bound superoxo species.¹⁶ For the lower-energy region, both the $^{16}\text{O}_2$ and $^{18}\text{O}_2$ data showed two peaks with an intensity distribution that changed with isotope. Therefore, these are both mixed as a result of Fermi resonance. Analysis¹⁵ of the lower-energy region (Figure 2A) showed a Cu– ^{16}O stretch at 482 cm^{-1} that was shifted to 462 cm^{-1} with ^{18}O .¹⁷

Thus, the rR spectroscopic data confirmed the formulation of $[\text{LCu}^{\text{II}}(\text{O}_2^{\bullet-})]^+$ as an end-on superoxo-containing complex with O–O and Cu–O stretches of 1130 and 482 cm^{-1} , respectively.¹⁵ Notably, these values are higher than those found for all cupric superoxo complexes previously described: $\nu(\text{O}-\text{O})$ for the one structurally defined side-on bound cupric superoxo complex is 1043 cm^{-1} , while those for the end-on bound species range up to 1122 cm^{-1} ; $\nu(\text{Cu}-\text{O})$ varies from 422 to 474 cm^{-1} .¹⁵ Using DFT calculations, we evaluated the Cu–O and O–O vibrational frequencies of **1**, a related structure having the pivalamido group at the para position instead of the ortho position, and a structure with Cu–N bonds constrained but no pivalamido group.¹⁵ The comparison between para and ortho substitution eliminated an inductive effect from the pivalamido group as the origin of the higher frequencies. Consistent with the $\nu(\text{O}-\text{O})$ of 1130 cm^{-1} , **1** was calculated to be an end-on bound Cu(II) superoxo species with a triplet ground state (the singlet/triplet splitting was calculated to be 1581 cm^{-1} ,¹⁵ after correction for spin contamination). For **L** and its close analogues, Masuda and co-workers^{14a} found that the pivalamidopyridyl substituent forms intramolecular H-bonds to the α oxygen atoms of a peroxide and/or hydroperoxide moiety ligated to the copper(II) ion^{14a,18} or to the α nitrogen atom of an azide coordinated to copper(II).^{14a} However, our calculations¹⁵ suggested that the superoxo moiety in $[\text{LCu}^{\text{II}}(\text{O}_2^{\bullet-})]^+$ (**1**) forms an intramolecular H-bond with either the α or β oxygen. This would contribute to the relative stability of **1** and can account for the higher O–O and Cu–O frequencies. rR data on the analogues $[\text{Cu}^{\text{II}}(\text{TMPA})(\text{O}_2^{\bullet-})]^+$ [TMPA = tris(2-pyridylmethyl)amine] and $[\text{Cu}^{\text{II}}(\text{NMe}_2\text{-TMPA})(\text{O}_2^{\bullet-})]^+$ show

a $\nu(\text{O}-\text{O})$ of 1120 cm^{-1} and a $\nu(\text{Cu}-\text{O})$ of 472 cm^{-1} ,¹² thus, $\nu(\text{O}-\text{O})$ and $\nu(\text{Cu}-\text{O})$ are both $\sim 10 \text{ cm}^{-1}$ higher in **1**. Optimized geometries of $[\text{Cu}^{\text{II}}\text{TMPA}(\text{O}_2^{\bullet-})]^+$ and $[\text{Cu}^{\text{II}}(\text{NMe}_2\text{-TMPA})(\text{O}_2^{\bullet-})]^+$ were also obtained through DFT calculations and compared to that of **1**. These calculations gave an increase in both $\nu(\text{Cu}-\text{O})$ and $\nu(\text{O}-\text{O})$ when H-bonding, particularly to the β oxygen of the superoxo ligand, was included in **1**.^{15,19} The calculated structure showed a decrease of 0.005 \AA in the Cu–O bond length, indicating that a slightly stronger Cu–O bond is associated with the higher $\nu(\text{Cu}-\text{O})$. From the DFT calculation of the structure with Cu–N bond lengths constrained at the values of the optimized structure of **1** but with no pivalamido group, this appears to reflect a distortion of the $\text{N}_{\text{equatorial}}$ ligand system that decreases its donor interaction with the Cu. The donor interaction of the superoxo with the Cu thus increases, leading to a stronger Cu–O bond. Alternatively, the calculations showed that the O–O bond length actually increases by 0.005 \AA in **1**, indicating that the increase in $\nu(\text{O}-\text{O})$ relative to $[\text{Cu}^{\text{II}}\text{TMPA}(\text{O}_2^{\bullet-})]^+$ does not reflect a stronger O–O bond but derives from structural coupling of vibrations within the ligand system due to the H-bond. This H-bonding stabilizes the superoxo species (relative to the binuclear peroxo species) and allows its reactivity to be studied.

$[\text{LCu}^{\text{II}}(\text{O}_2^{\bullet-})]^+$ (**1**) is unreactive toward a number of commonly employed C–H substrates, such as dihydroanthracene, xanthene, and 10-methyl-9,10-dihydroacridine, which are substrates possessing C–H bonds that are significantly weaker than those found for the D β M and PHM substrates (dopamine, 85 kcal/mol ; hippuric acid, 87 kcal/mol).^{6b} However, the addition of an excess of 1-benzyl-1,4-dihydropyridinamide (**BNAH**), an NADH analogue that is both a strong H atom (H^\bullet) and hydride (H^-) donor,¹⁹ to solutions of $[\text{LCu}^{\text{II}}(\text{O}_2^{\bullet-})]^+$ leads to the decay of the latter, as observed by UV–vis spectroscopy (Figure 3a). Kinetic interrogation of this reaction ($-125 \text{ }^\circ\text{C}$) showed pseudo-first-order decay behavior with respect to **1** (for 10–40 equiv of **BNAH**). The decay was also first-order in $[\text{BNAH}]$. Thus, the cupric superoxo complex is responsible for promoting the substrate oxidation (see below). A second-order rate constant of $0.19 \text{ M}^{-1} \text{ s}^{-1}$ was obtained (Figure 3b); when the substrate was deuterated in the 4 and 4' positions, i.e., when 1-benzyl-1,4-dihydro[4,4'- $^2\text{H}_2$]nicotinamide (**BNAD**) was used, a significant slowing of the reaction occurred ($k = 0.016 \text{ M}^{-1} \text{ s}^{-1}$; Figure 3b). This gives a kinetic isotope effect (KIE) of 12.1. This KIE value is comparable to the KIE of 10 reported for C–H bond cleavage of **BNAH** by a *trans*-dioxomanganese(V) porphyrin.²⁰ Product analysis of the $[\text{LCu}^{\text{II}}(\text{O}_2^{\bullet-})]^+/\text{BNAH}$ reaction (following quenching with HCl at $-130 \text{ }^\circ\text{C}$)¹⁵ confirmed that **BNAH** underwent oxidation by **1**. The substrate's 4' C–H bond was oxidatively cleaved to form 1-benzylnicotinamidium ion (**BNA⁺**) in 42% yield (^1H NMR) based on the initial copper concentration (Scheme 1). Additionally, upon acidification, liberated hydrogen peroxide was also detected in $\sim 30\%$ yield, approximately corresponding to the amount of the peroxodicopper(II) complex $[\{\text{LCu}^{\text{II}}\}_2(\text{O}_2^{2-})]^{2+}$ (**2**), which was also a reaction product as identified by its characteristic UV–vis absorption bands (see above).

Cupric superoxo-promoted cleavage of the C–H bond likely follows one of two possible pathways (Scheme 1). One is initial H-atom transfer (HAT), in which the C–H bond is cleaved homolytically (with the thus-formed **BNA** radical rapidly losing a second electron); the other involves hydride transfer resulting from heterolytic cleavage. To provide further mechanistic insight

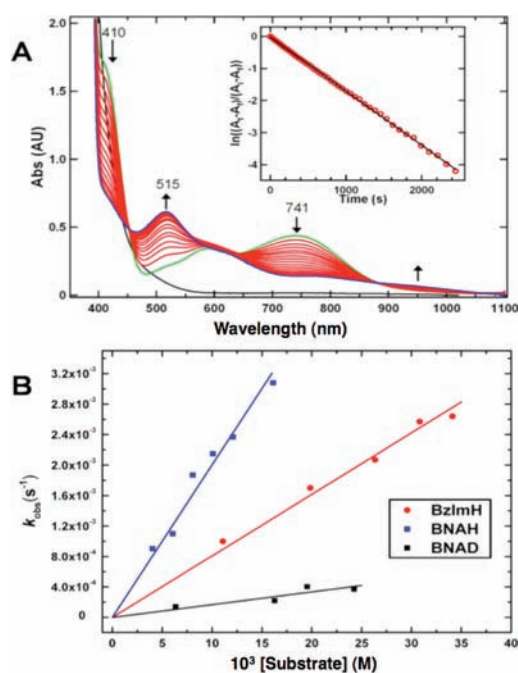


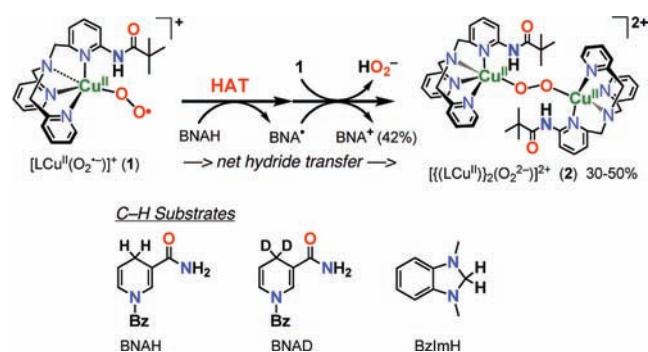
Figure 3. (a) Spectral changes of 0.4 mM $[\text{LCu}^{\text{II}}(\text{O}_2^{\bullet-})]^+$ in the presence of 8 mM **BNAH** at $-125\text{ }^\circ\text{C}$ in MeTHF. The first spectrum recorded (green) is that immediately following bubbling of O_2 through a solution containing $[\text{LCu}^{\text{I}}]^+$ and **BNAH**. Inset: pseudo-first-order kinetics fit of the 741 nm data. (b) Plots of k_{obs} as a function of **BNAH**, **BNAD**, or **BzImH** concentration, used to determine the second-order rate constants.

into the mode of C–H activation by **1**, a second substrate, 1,3-dimethyl-2,3-dihydrobenzimidazole (**BzImH**),²¹ was studied for reactivity. Like **BNAH**, **BzImH** possesses a weak C–H bond but has markedly different bond strengths than **BNAH** (homolytic, bond dissociation energy = 73.4 kcal/mol vs 70.7 kcal/mol for **BNAH**; heterolytic, hydride affinity = 49.5 kcal/mol vs 64.2 kcal/mol for **BNAH**).²¹ Kinetic studies revealed that the oxidation of **BzImH** occurs ~ 2.4 times slower than that of **BNAH**, with a second-order rate constant of $0.078\text{ M}^{-1}\text{ s}^{-1}$ (Figure 3b). The lower rate of C–H oxidation of **BzImH** (stronger H^- donor) than of **BNAH** (stronger H^\bullet donor) thus suggests that at least for these substrates, the preferred mode of C–H activation by $[\text{LCu}^{\text{II}}(\text{O}_2^{\bullet-})]^+$ is via rate-limiting homolytic C–H bond cleavage, i.e., HAT.

On the basis of extensive studies of the enzymes PHM and $D\beta\text{M}$, the most accepted mechanistic proposal is that these enzymes initially proceed by (nonclassical)^{6b,22} HAT chemistry promoted by a cupric superoxo complex generated at the Cu_{M} site.^{8a,9a} Interestingly, enzyme kinetic studies carried out on $D\beta\text{M}$ and PHM revealed KIEs of 10–14.^{6,23} (depending on the conditions), which are very similar to that found here for our system. The studies reported here with a “model” cupric superoxide complex suggest that this mechanism is followed, at least for the relatively weak C–H substrates investigated. In one case, theoretical calculations inspired by results on a model system led to the suggestion that an initial hydride abstraction may occur for PHM/ $D\beta\text{M}$.²⁴ The present findings suggest that this is not likely to be a favorable pathway.

Following C–H activation, the overall mechanism of substrate hydroxylation by the enzymes $D\beta\text{M}$ and PHM is poorly understood, with nearly as many proposals for the subsequent

Scheme 1



steps as there are researchers in the field.¹⁵ The steps to products following the transition state are also difficult to surmise in our chemical systems.²⁵ Despite these uncertainties, the importance of the present studies lies in the observation of intermolecular C–H activation by a cupric superoxo complex.

To summarize, a new ligand-supported cupric superoxo complex with reactivity behavior of relevance to the $D\beta\text{M}$ and PHM enzymes has been described. Significant advances include the following: (a) $[\text{LCu}^{\text{II}}(\text{O}_2^{\bullet-})]^+$ (**1**) is the first cupric superoxo complex that incorporates a hydrogen-bonding ligand feature. (b) This results in a compound with stronger Cu–O and O–O bonds than in previously known examples. (c) Not necessarily related to the latter properties, the reactions of **1** with **BNAH** and **BzImH** provide the first examples of intermolecular C–H bond activation by a cupric superoxo complex. Notably, it is not unexpected that relatively weak C–H bonds are cleaved for an intermolecular situation; one does not have the advantage of a proximate substrate, as found for the single known example of intramolecular $\text{Cu}^{\text{II}}(\text{O}_2^{\bullet-})$ -mediated C–H oxidation.¹³ (d) Finally, the relative rates for C–H oxidation of these two substrates support rate-limiting homolytic C–H bond activation. Further corroborating studies with other C–H mechanistic probes will be investigated. The clean kinetic behavior, striking deuterium KIE, and determination of rate-limiting HAT demonstrate that the reaction of $[\text{LCu}^{\text{II}}(\text{O}_2^{\bullet-})]^+$ (**1**) with C–H substrates may possess biological significance in direct comparison to the reaction mechanism of the $D\beta\text{M}$ and PHM enzymes.

■ ASSOCIATED CONTENT

S Supporting Information. Experimental procedures, spectra, DFT calculations, explanations and supporting diagrams, and crystallographic data (CIF). This material is available free of charge via the Internet at <http://pubs.acs.org>.

■ AUTHOR INFORMATION

Corresponding Author

edward.solomon@stanford.edu; fukuzumi@chem.eng.osaka-u.ac.jp; karlin@jhu.edu

■ ACKNOWLEDGMENT

This research was supported by the National Institutes of Health (GM28962 to K.D.K. and DK31450 to E.I.S.), WCU Program R31-2008-000-10010-0 (to K.D.K. and S.F.), by a

Grant-in-Aid 20108010 (S.F.), and the Global COE Program from the Ministry of Education, Culture, Sports, Science and Technology, Japan (S.F.)

REFERENCES

- (1) (a) Holm, R. H.; Kennepohl, P.; Solomon, E. I. *Chem. Rev.* **1996**, *96*, 2239–2314. (b) Solomon, E. I.; Chen, P.; Metz, M.; Lee, S.-K.; Palmer, A. E. *Angew. Chem., Int. Ed.* **2001**, *40*, 4570–4590.
- (2) (a) Mirica, L. M.; Ottenwaelder, X.; Stack, T. D. P. *Chem. Rev.* **2004**, *104*, 1013–1045. (b) Lewis, E. A.; Tolman, W. B. *Chem. Rev.* **2004**, *104*, 1047–1076.
- (3) Itoh, S. *Curr. Opin. Chem. Biol.* **2006**, *10*, 115–122.
- (4) (a) Quant Hatcher, L.; Karlin, K. D. *J. Biol. Inorg. Chem.* **2004**, *9*, 669–683. (b) Himes, R. A.; Karlin, K. D. *Curr. Opin. Chem. Biol.* **2009**, *13*, 119–131.
- (5) Cramer, C. J.; Tolman, W. B. *Acc. Chem. Res.* **2007**, *40*, 601–608.
- (6) (a) Klinman, J. P. *Chem. Rev.* **1996**, *96*, 2541–2561. (b) Klinman, J. P. *J. Biol. Chem.* **2006**, *281*, 3013–3016. (c) Prigge, S. T.; Eipper, B. A.; Mains, R. E.; Amzel, L. M. *Science* **2004**, *304*, 864–867.
- (7) Chen, P.; Solomon, E. I. *Proc. Natl. Acad. Sci. U.S.A.* **2004**, *101*, 13105–13110.
- (8) (a) Evans, J. P.; Ahn, K.; Klinman, J. P. *J. Biol. Chem.* **2003**, *278*, 49691–49698. (b) Bauman, A. T.; Yukl, E. T.; Alkevich, K.; McCormack, A. L.; Blackburn, N. J. *J. Biol. Chem.* **2006**, *281*, 4190–4198.
- (9) (a) Chen, P.; Solomon, E. I. *J. Am. Chem. Soc.* **2004**, *126*, 4991–5000. (b) Chen, P.; Bell, J.; Eipper, B. A.; Solomon, E. I. *Biochemistry* **2004**, *43*, 5735–5747. (c) Comba, P.; Knoppe, S.; Martin, B.; Rajaraman, G.; Rolli, C.; Shapiro, B.; Stork, T. *Chem.—Eur. J.* **2008**, *14*, 344–357.
- (10) (a) Maiti, D.; Lee, D.-H.; Gaoutchenova, K.; Würtele, C.; Holthausen, M. C.; Narducci Sarjeant, A. A.; Sundermeyer, J.; Schindler, S.; Karlin, K. D. *Angew. Chem., Int. Ed.* **2008**, *47*, 82–85. (b) Maiti, D.; Narducci Sarjeant, A. A.; Karlin, K. D. *Inorg. Chem.* **2008**, *47*, 8736–8747.
- (11) (a) Decker, A.; Solomon, E. I. *Curr. Opin. Chem. Biol.* **2005**, *9*, 152–163. (b) Yoshizawa, K.; Kihara, N.; Kamachi, T.; Shiota, Y. *Inorg. Chem.* **2006**, *45*, 3034–3041. (c) Crespo, A.; Martí, M. A.; Roitberg, A. E.; Amzel, L. M.; Estrin, D. A. *J. Am. Chem. Soc.* **2006**, *128*, 12817–12828. (d) Huber, S. M.; Ertem, M. Z.; Aquilante, F.; Gagliardi, L.; Tolman, W. B.; Cramer, C. J. *Chem.—Eur. J.* **2009**, *15*, 4886–4895.
- (12) Maiti, D.; Fry, H. C.; Woertink, J. S.; Vance, M. A.; Solomon, E. I.; Karlin, K. D. *J. Am. Chem. Soc.* **2007**, *129*, 264–265.
- (13) Kunishita, A.; Kubo, M.; Sugimoto, H.; Ogura, T.; Sato, K.; Takui, T.; Itoh, S. *J. Am. Chem. Soc.* **2009**, *131*, 2788–2789.
- (14) (a) Yamaguchi, S.; Wada, A.; Funahashi, Y.; Nagatomo, S.; Kitagawa, T.; Jitsukawa, K.; Masuda, H. *Eur. J. Inorg. Chem.* **2003**, 4378–4386. (b) $[(\text{LCu}^{\text{II}})_2(\text{O}_2^{2-})]^{2+}$ (**2**) possesses distinctive UV–vis absorptions and a $\nu(\text{O}—\text{O})$ of 837 cm^{-1} .
- (15) See the Supporting Information.
- (16) The complex formed with $^{18}\text{O}_2$ had a small $^{16}\text{O}_2$ contamination estimated to be 18% from the weak O—O feature at 1130 cm^{-1} observed in the ^{18}O sample spectrum. The signal of the ^{16}O sample was scaled and subtracted from the ^{18}O spectrum in the analysis of the Cu— ^{18}O vibrational region.
- (17) A resonance-enhanced peak at 485 cm^{-1} was observed for the complex formed with $^{16}\text{O}_2$, together with a less intense peak at 452 cm^{-1} . For the complex formed with $^{18}\text{O}_2$, two peaks were observed at 468 and 448 cm^{-1} , with their relative intensities reversed in comparison with the spectrum of the ^{16}O sample. This pattern also indicates a Fermi resonance with a nonenhanced mode at similar energy, in this case for both the Cu— ^{16}O and Cu— ^{18}O spectra. From the analysis (see the Supporting Information), the preinteraction Cu—O stretching frequency for the ^{16}O complex is at 482 cm^{-1} and that for the ^{18}O complex is at 462 cm^{-1} .
- (18) Wada, A.; Harata, M.; Hasegawa, K.; Jitsukawa, K.; Masuda, H.; Mukai, M.; Kitagawa, T.; Einaga, H. *Angew. Chem., Int. Ed.* **1998**, *37*, 798–799.
- (19) (a) Fukuzumi, S.; Koumitsu, S.; Hironaka, K.; Tanaka, T. *J. Am. Chem. Soc.* **1987**, *109*, 305–316. (b) Yuasa, J.; Fukuzumi, S. *J. Am. Chem. Soc.* **2006**, *128*, 14281–14293.
- (20) Lee, J. Y.; Lee, Y.-M.; Kotani, H.; Nam, W.; Fukuzumi, S. *Chem. Commun.* **2009**, 704–706.
- (21) Zhu, X.-Q.; Zhang, M.-T.; Yu, A.; Wang, C.-H.; Cheng, J.-P. *J. Am. Chem. Soc.* **2008**, *130*, 2501–2516.
- (22) Francisco, W. A.; Blackburn, N. J.; Klinman, J. P. *Biochemistry* **2003**, *42*, 1813–1819.
- (23) Bollinger, J. M., Jr.; Krebs, C. *Curr. Opin. Chem. Biol.* **2007**, *11*, 151–158.
- (24) de la Lande, A.; Parisel, O.; Gérard, H.; Moliner, V.; Reinaud, O. *Chem.—Eur. J.* **2008**, *14*, 6465–6473.
- (25) For **BNAH**, no organic products besides **BNA⁺** were detected in the reaction mixture. The sole inorganic product identified was the *trans*-peroxo complex **2**, though it accounted for only ~50% of the total copper content in the reaction. Several pathways that lead to **2** following sequential HAT/electron transfer to **1** may be envisioned, giving a putative Cu(I)—OOH moiety that could “trap” an equivalent of **1** to give **2** and HO_2^- . This would lead to consumption of 2 equiv of **1** per equivalent of substrate and explain the close-to-50% (as opposed to quantitative) yield of **BNA⁺**. The *trans*-peroxo species **2** was not reactive toward **BNAH** at $-125\text{ }^\circ\text{C}$ and decomposed only very slowly in the presence of large excesses of **BzImH**. Further incubation of the final reaction mixture did not lead to higher detected yields of **BNA⁺**, i.e., other copper species present following the conclusion of the reaction did not react with the substrate at the temperature examined.